

Final Report  
Contract H31548D

Raymond A. Lewis  
1308 Andover Drive  
Boalsburg, PA 16827

814 466 6187  
814 423 2583 (fax)

[r3l@psu.edu](mailto:r3l@psu.edu)

March 13, 2001

March 13, 2001  
RAL

## Antimatter/HiPAT Support Services

### Overview

Techniques were developed for trapping normal matter in the High Performance Antiproton Trap (HiPAT). Situations encountered included discharge phenomena, charge exchange and radial diffusion processes. It is important to identify these problems, since they will also limit the performance in trapping antimatter next year. The HiPAT hardware is illustrated in Figure 1.

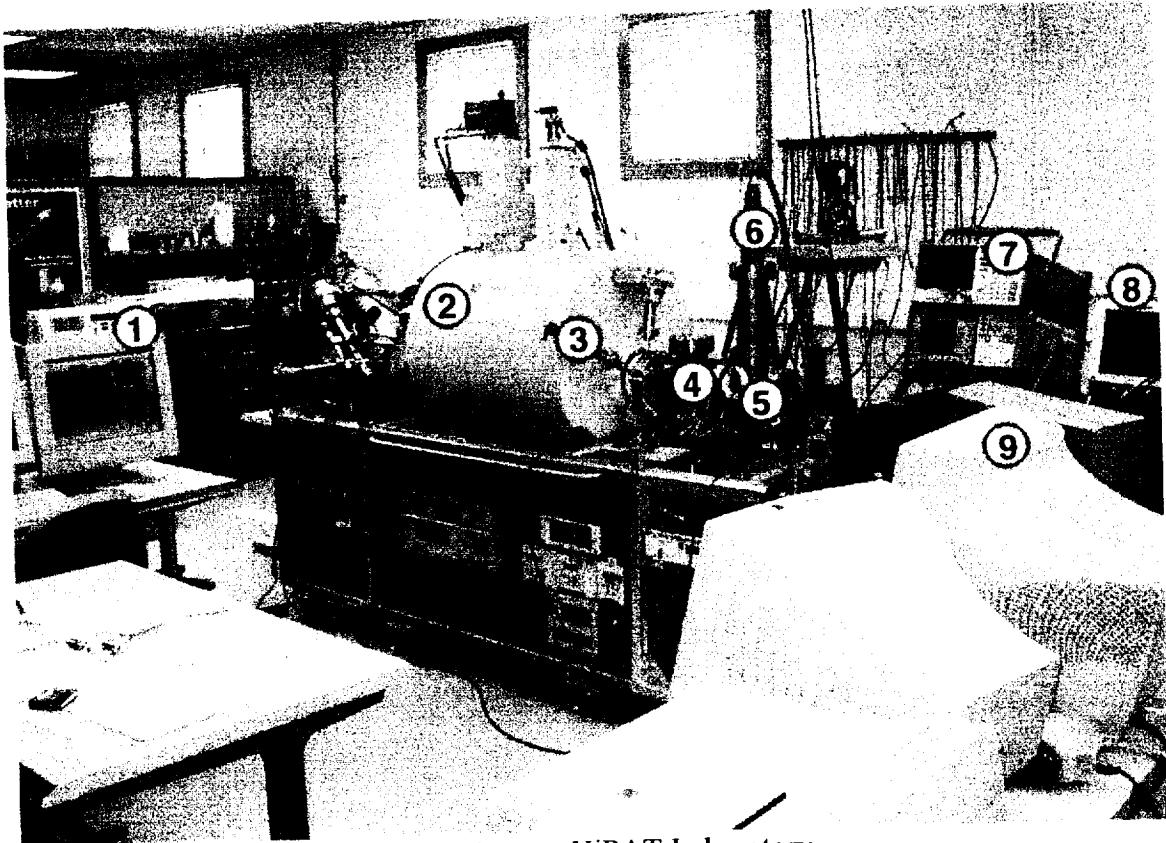


Figure 1 HiPAT Laboratory

Figure 1 includes the following, from left to right:

1. Monitor showing the LabView display for controlling electrode voltages;
2. Liquid helium cryostat, containing a superconducting coil (4 Tesla) and the trap inside a vacuum pipe;
3. Micro-channel plate (MCP) detector, mounted on a motion feedthrough;
4. Solenoids around the beampipe, for guiding an electron beam into the trap;
5. A 90° bend dipole magnet;
6. An electron gun.
7. Two spectrum analyzers, for generating radio frequency (RF) and detecting RF from the trap;

8. Storage scope, for recording signals from the MCP;
9. Monitors for recording data from the storage scope.

The labeling of the electrodes in the trap is shown in figure 2, and an illustration of the trapping region with applied fields is shown in figure 3. The picture of the electrodes in figure 4 shows the arrangement of Macor insulation, and kapton wiring.

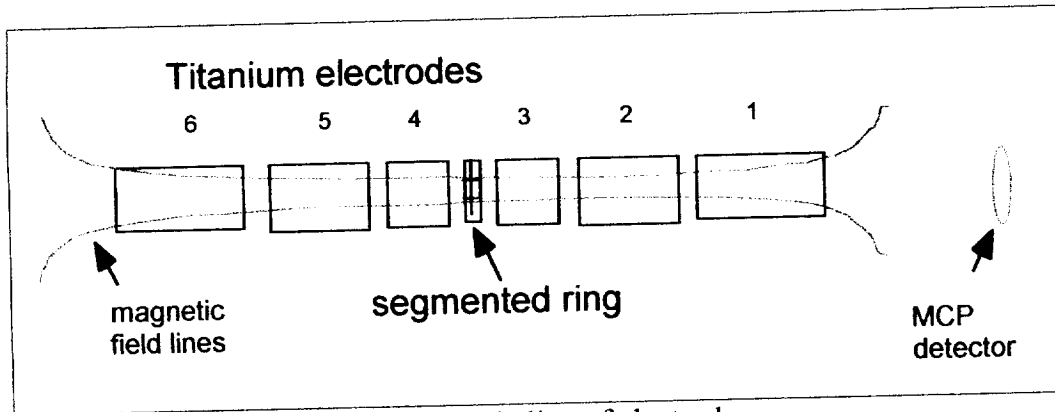


Figure 2 Labeling of electrodes.

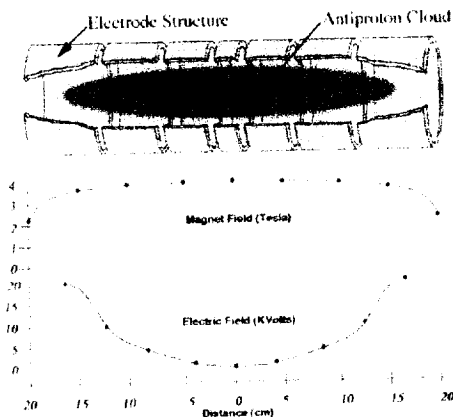


Figure 3 Magnetic field & potential well.

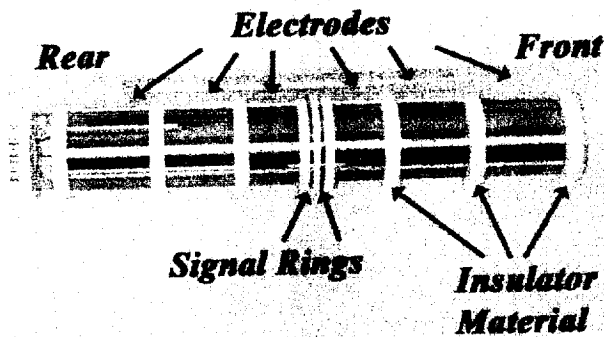


Figure 4 Photograph of trap electrodes

Particles are confined radially by the axial magnetic field. Axial confinement is imposed by applying voltages onto the cylindrical electrodes, forming a potential well. Particles are dumped from the trap by lowering the potentials on electrodes 1,2,3, either rapidly (100 nsec) for a fast dump, or slowly over a period of several seconds.

The RF from the generator is split into four phases, and imposed on 4 of the 8 segments of the ring electrode, forming a rotating wall<sup>1</sup>. The remaining 4 segments are used for picking up currents induced by ions on the electrodes. These signals are amplified, and interpreted with a spectrum analyzer.

### Discharge phenomena

When the trap was first tried out, clouds of ions could not be stored reliably. An attempt was made to load the trap with electrons, which should have been detected

passively, using resonant pickup circuitry<sup>2</sup>. Large signals were measured on the spectrum analyzer. Several of the preamps were “fried”, due to a runaway (Penning) discharge. The discharge is termed “pigging” in devices in which it is desirable, such as a Penning ion gauge.

When the trap was reconfigured to trap positive ions, the discharge problem persisted. Large signals were still present on the spectrum analyzer. Huge numbers (millions) of positive ions could be detected in an MCP upon extraction. However the trap would spontaneously refill, without the aid of an electron beam to create fresh ions. The problem was traced to the presence of “pockets” in the potential well, which trapped electrons. The electrons created ions by the pigging mechanism.

The discharge behavior was quenched, by mounting “spoiler” screens around the periphery of the end electrodes (1 and 6). The screens are floated to a high potential, to attract electrons. The shaping of the screen edges disrupts the pigging mechanism. Subsequent tests with the glow quenched showed no activity on the spectrum analyzer.

### Identification of discharge features

Optical techniques were used to identify background processes in the trap associated with a discharge.

By altering the biasing on the spoiler screens, Penning discharges could be made intense enough to produce a visible glow. The light from the glow discharge was analyzed with a spectrum analyzer. The hydrogen lines expected were rather weak, relative to a dozen stronger lines attributable to CO gas and CO<sup>+</sup> ions. Photographs with a CCD camera showed clear images with bright regions in the pockets which trap electrons, as shown in figure 5. Some of the CCD pictures showed streamers, resembling illustrations found in textbooks on the development of radar.

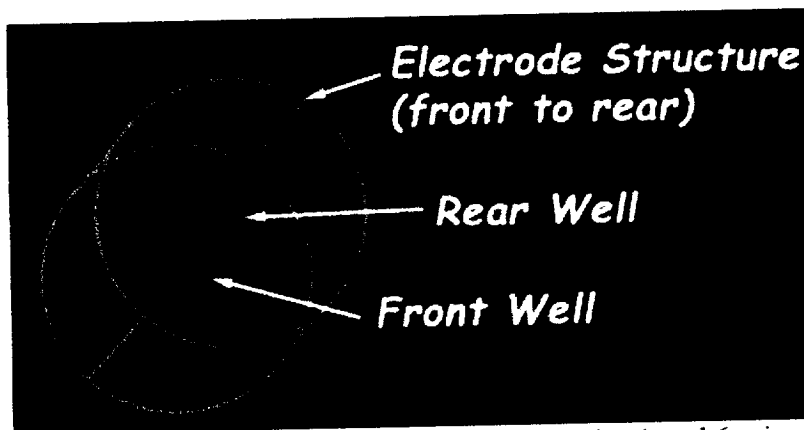


Figure 5 Photograph of glow regions centered in electrodes 1 and 6, viewed through a sight glass.

### Identification of charge exchange

With the discharge problem under control, reproducible results were obtained by dumping the trap contents onto an MCP detector. The three downstream electrodes of the trap are grounded rapidly, using a high-speed, high-voltage Behlke switch. The

timing pattern of signals obtained from the MCP indicates the time-of-flight (t.o.f.) of various ions from the trap.

Three well-defined signals were systematically found, with t.o.f.'s in the ratio of  $\sqrt{1}, \sqrt{2}, \sqrt{3}$ . The interpretation is that hydrogen ion clusters  $H^+, H_2^+$  and  $H_3^+$  were formed, and acquired the same kinetic energy upon ejection from the trap. The t.o.f.'s would then be in the ratio of the ion cluster masses. These same ion clusters have been observed in other devices, such as ion sources<sup>3</sup>.

After ions have been stored for tens of minutes, signals with much longer t.o.f. are observed in the MCP, as shown in figure 6. Assuming the pattern observed with the hydrogen ions, masses can be assigned to the later signals. The highest mass ion cluster observed consistently is  $CO_2^+$ , with a molecular weight of 44 amu. Other t.o.f. peaks are consistent with  $C^+, CH_2^+, H_2O^+, CO^+$  ions.

The number of ions indicated for each species is determined from the area of the peak, assuming a gain of  $10^6$  in the MCP. For a comparison, the  $3 \mu m$  radius region in which ions are created, defined by the electron beam, can contain 30,000  $H^+$  ions at the maximum density allowed by the Brillouin limit.

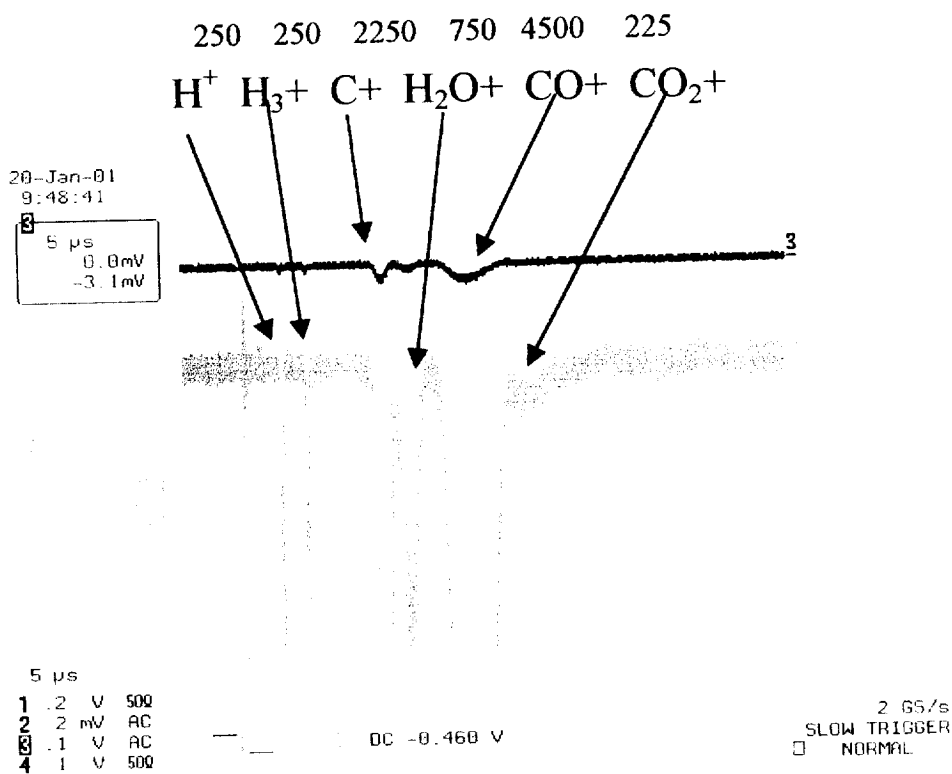


Figure 6 January 19, run 43--16 hours, with RF 15 dB, 400-500 kHz

The mechanism for producing the ions clusters is charge exchange<sup>3</sup>. The electron beam initially produces only H<sup>+</sup> ions. The background gas density is high (4\*10<sup>-10</sup> Torr) while the electron gun is firing, and contains sufficient H<sub>2</sub> gas for hydrogen charge-exchange to occur on a time scale of seconds. Other background gases, such as CO, H<sub>2</sub>O, CO<sub>2</sub>, are minority constituents. Most of the background gas in the 10<sup>-10</sup> Torr vacuum is hydrogen. However various ion clusters such as CO<sup>+</sup> have a lower energy than H<sup>+</sup>, so that on a time scale of hours mostly heavy ion clusters replace the hydrogen ions.

As a result of observing carbon compounds, various expertise was tapped, at Varian and Oak Ridge National Laboratory (ORNL). Following their suggestions, a new cleaning procedure involving plasma discharge is being engineered. Also titanium was selected to replace copper for the electrode material.

### Need for RF excitation

The t.o.f. data from the MCP are often ambiguous, with timing patterns varying by several  $\mu$ sec depending on holding time. Another tool is needed, to identify what species of ions and energy states exist in the trap.

Antiprotons have been stored in a small, sealed cryogenic vacuum Penning trap for several months<sup>4</sup>. These conditions cannot be met with HiPAT, which is designed to hold billions of particles, with connections to an external beamline for injection and extraction. Some type of stabilization is anticipated, to overcome the problems associated with inter-particle interactions (space charge effects), as well as a degraded vacuum due to the open geometry.

In addition to diagnostics, RF has also been reported as a stabilization agent. Large clouds of ions have been stored for periods of weeks, using several stabilization schemes.

### Cyclotron heating

The cyclotron frequency for an ion species with mass M is related to the magnetic field,

$$\omega_c = qB/M \quad \text{Eqn. (1),}$$

where B is the magnetic field strength, q the ion charge. Unlike the t.o.f. information, the cyclotron frequency is independent of the energy of the ion, depending only on the mass/charge ratio. The cyclotron data is complementary to the MCP t.o.f. data.

Besides its use as a diagnostic tool, cyclotron resonance heating has also been reported<sup>5</sup> as a stabilization technique. The technique bears a superficial resemblance to magnetron centering<sup>6</sup>, in which RF at a frequency slightly above the cyclotron frequency drives a few particles towards the symmetry axis of the trap. In the Isoltrap application to a large cloud of ions, frequencies in a broad ( $\pm 5\%$ ) band either above or below the cyclotron frequency are effective in providing compression.

Evidence for cyclotron excitation has been observed in HiPAT. Figure 6 shows a typical MCP spectrum and its interpretation. The yields of the various ion species vary as the frequency of RF excitation is varied, as shown in figure 7. The striking feature of figure 7 is that ion species are selectively expelled from the trap, with frequencies listed in table 1.

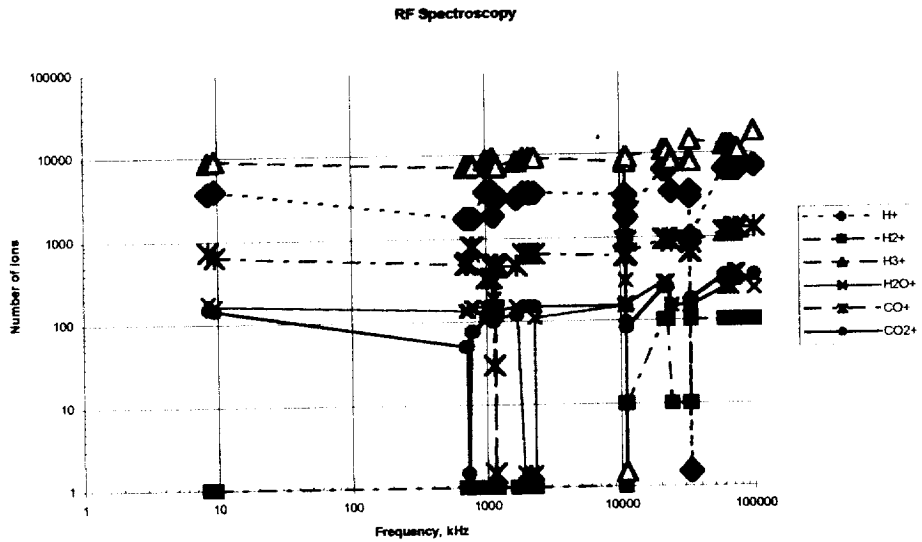


Figure 7 Effect of RF frequency on various ion species.

Table 1 List of frequencies which expel various ion species

Ion species	r.f. frequency
H <sup>+</sup>	33.213 to 33.288 MHz
H <sub>2</sub> <sup>+</sup>	NA
H <sub>3</sub> <sup>+</sup>	10.996 to 11.096 MHz
H <sub>2</sub> O <sup>+</sup>	1690 to 1720 kHz
CO <sup>+</sup>	1140 to 1150 kHz
CO <sub>2</sub> <sup>+</sup>	725 to 740 kHz

While the H<sub>2</sub><sup>+</sup> signal is usually small, it shows up strongly when the RF is tuned to expel H<sub>3</sub><sup>+</sup> ions. Figure 3 shows a plot of the active frequencies versus ion cluster mass.

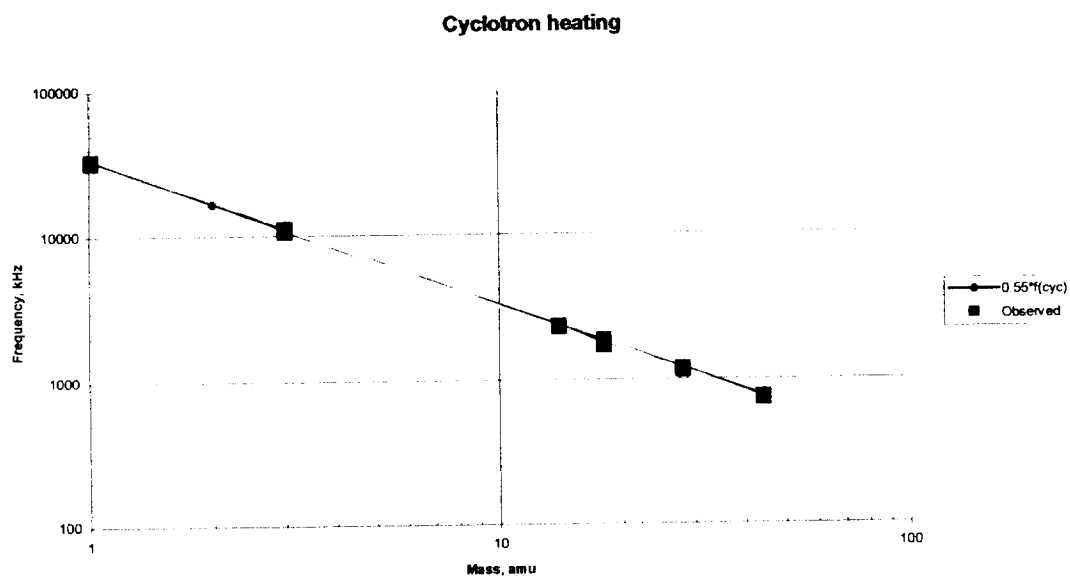


Figure 8 Cyclotron heating frequency versus ion cluster mass

The active frequency for a given ion species is  $0.55 \pm 0.02$  times its predicted cyclotron frequency. The error bars represent day-to-day variations.

The error bars are small enough to use the technique to identify ions which are ambiguous in their t.o.f. signals. For example, the  $\text{H}_2\text{O}^+$  ions extracted from the trap show up with t.o.f. ranging from 14 to 16  $\mu\text{sec}$ , corresponding to variations between 100 and 70 eV kinetic energy. The cyclotron resonance technique identified the ions as  $\text{H}_2\text{O}^+$ . This leads to a scenario in which  $\text{H}_2\text{O}^+$  ions reside in the trap, in energy states ranging from 70 to 100 eV above ground. Alternative hypotheses, such as a transformation involving  $\text{H}_3\text{O}^+$  ions<sup>7</sup>, are ruled out by observing a continuous variation between 14 and 16  $\mu\text{sec}$ , as the holding time is varied.

### Evidence for sharply-defined energy states

Evidence that the signal which migrates between 14 and 16  $\mu\text{sec}$  is attributable to a continuous parameter (energy), rather than a discrete parameter (e.g. accumulating H atoms to form clusters such as  $\text{H}_3\text{O}^+$ ) is shown in a series of runs with varying hold times. The figure below shows the migrating peak near 15  $\mu\text{sec}$ , after a holding time of 12.5 minutes.

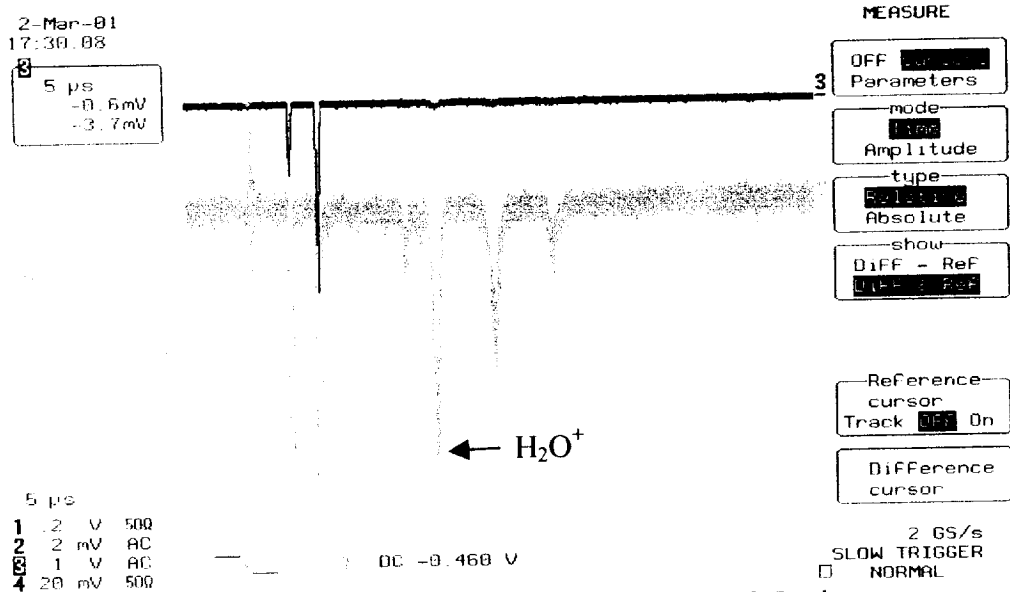


Figure 9 March 2 run 28, no RF, 12.5 minutes

The energy states are sharply defined, with a few eV energy spread, as judged from the sharpness ( $< 1 \mu\text{sec}$  FWHM) of the t.o.f. lines. The best explanation is that under certain conditions, the  $\text{H}_2\text{O}^+$  ions are nudged away from the symmetry axis, into a lower potential energy region at larger radius. A related centrifugal separation<sup>8</sup> has been observed in other traps, wherein heavy and light mass ions migrate to different radial layers.

**Stabilization with RF at the cloud rotation frequency**

The use of a rotating wall<sup>9</sup> was developed at UCSD. In a steady state, all ions in a cloud rotate about the symmetry axis at a common angular velocity, which increases as the density of the ions increases. A rotating electric field, created by applying RF at different phases to a segmented electrode, is used to speed up the cloud rotation, and hence compress the cloud to higher density. By leaving the RF excitation on, the technique also increases the lifetime of the cloud. In the absence of RF stabilization, a cloud of ions slowly expands radially, due to collisions with background gas and to perturbations arising from mechanical misalignments between the electric and magnetic field symmetry axes.

Appropriate RF frequencies for stabilizing ions in HiPAT were found empirically. A guideline for finding a useful cloud rotation frequency involves the Brillouin limit. The cloud rotation frequency must be less than half the cyclotron frequency, in order for magnetic confinement forces to exceed space charge repulsion. The cyclotron frequency for the heaviest component,  $\text{CO}_2^+$ , is around 1 MHz, so that this component would be unstable with rotation frequencies above about  $\frac{1}{2}$  MHz. Having a ballpark estimate for the RF frequency is important, since the stabilizing effects of RF show up only after many hours of holding time.

Figures 10 and 11 below illustrate the stabilizing effect of RF, with frequency swept continuously between 0.4 and 0.5 MHz. Without RF, most of the ions have diffused out of the trap in 40 hours.

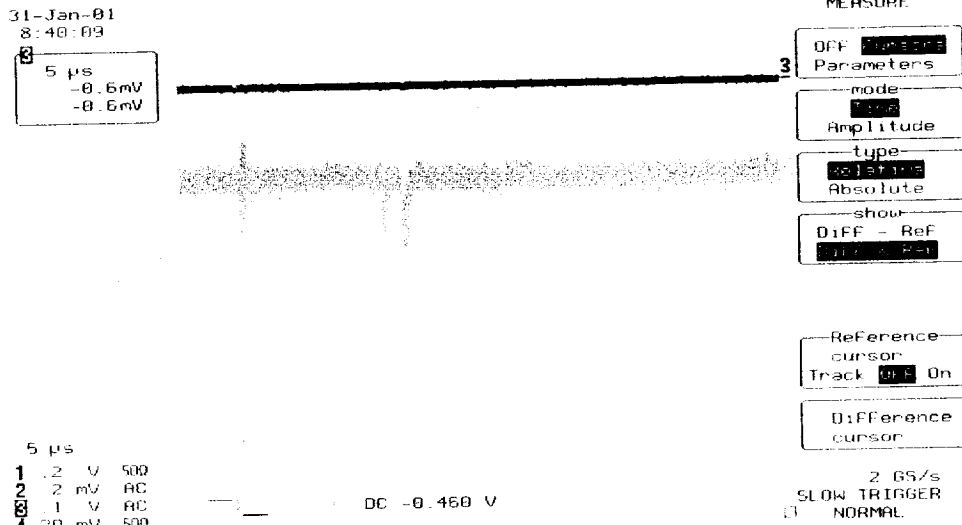


Figure 10 Jan29Run 19 -- hold for 40 hours, no RF

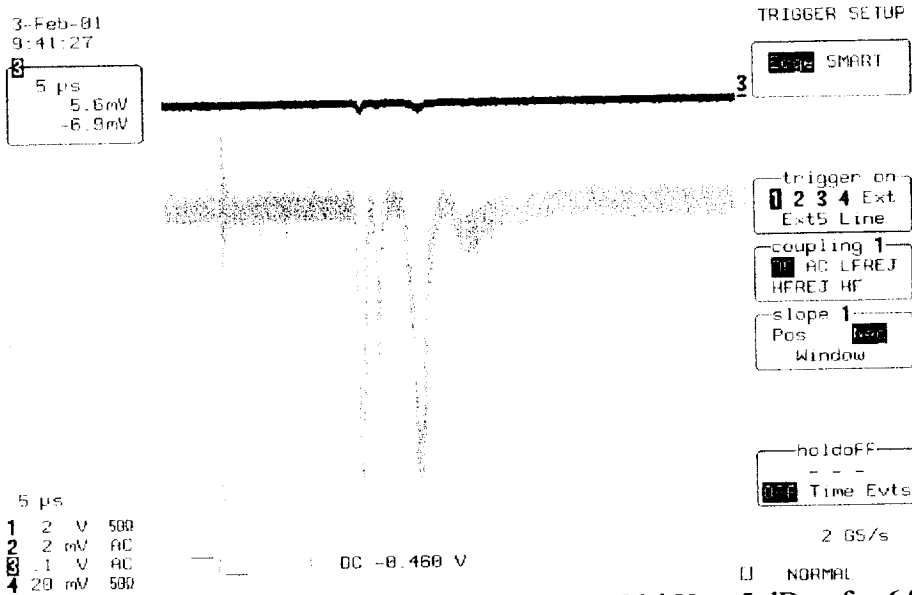


Figure 11 Jan31Run 43 -- RF 400-500 kHz, -5 dBm, for 64 hours.

With the RF stabilization, roughly 2400 ions remained in the trap for 64 hours. This yield is a major fraction of the 15,000 ions extracted after holding times of a few minutes.

As illustrated in figure 12, the RF stabilization increases the ion cloud lifetime by a factor of 4.5, from 9.5 to 43 hours.

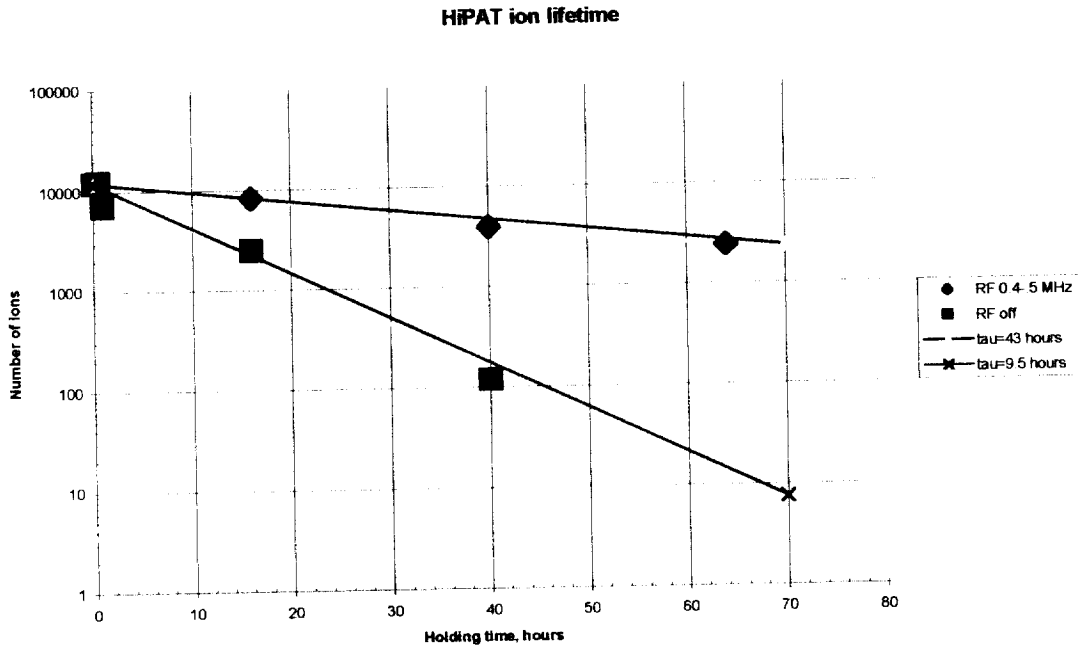


Figure 12 Ion yield versus storage time.

### Axial resonances

The split ring electrode was segmented into 4 azimuthal and 2 axial sectors. The reasoning was that under some circumstances axial motion is more readily sensed than is rotational motion.

Scans have been made with a spectrum analyzer, for signals with frequencies between the cloud rotation and cyclotron frequencies, indicating axial motion. The search was refined, by using electrodes 3 and 4 to get more sensitivity to axial motion, without an admixture of rotational signals.

After fixing the problems with plasma discharge, no signals from ion motion inducing currents in the electrodes have been observed. This aspect of the project will need to be pursued, since passive detection will be a useful component of transporting antimatter.

### Slow extraction

So far the most useful diagnostic tool involves a fast extraction. A Behlke switch grounds the three end electrodes, in a time scale of tens of nanoseconds. The time information recorded in the MCP is related to the velocity of ions extracted from the trap.

In a slow extraction, the voltages on the three end electrodes are reduced slowly, on a time scale of seconds. The time information in the MCP is related to the energy of particles in the trap. Ions with the highest kinetic energy emerge first, when the voltage ramped down. Colder ions emerge later. All ions should be extracted eventually, when the potential well barrier is reduced to zero.

Very few ions are observed with the slow dump technique, probably due to beam instability in the diverging magnetic field at the end of the trap.

A motivation for developing the slow extraction is that this technique proved valuable in trapping antiprotons at CERN. Figure 13 below<sup>10</sup> shows the yield versus time from a

typical run. The highest energy (28.5 keV) antiprotons are earliest, with energies down to zero emerging at the end of the 600 msec ramp. The general shape of the energy spectrum shows that antiprotons have started to cool. The sharp peaks, indicating some kind of clustering effect, have not been explained.

The energy clustering effect might be related to recent observations in HiPAT, described above in relation to fast extraction of  $H_2O^+$  ions.

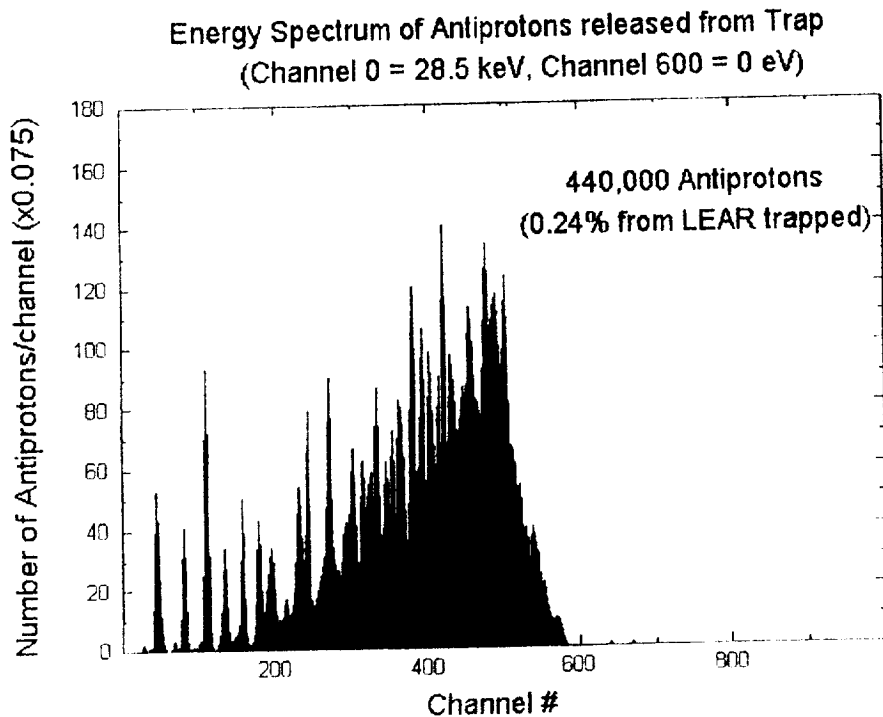


Figure 13 Slow extraction of antiprotons, CERN PS200. (1 channel=1 msec).

### ***Relevance to antiproton trapping***

The main goal for the near future is to facilitate the process of filling the trap with antimatter, and holding it for long periods of time.

The scattering and alignment effects apply to both matter and antimatter storage. The stabilizing effect of RF in the 0.5 MHz range should be directly applicable to antiprotons. Even the chemistry has an analogue—the cross sections for antiproton-atom formation<sup>11</sup> at low energy are comparable to the Gbarn charge-exchange cross sections among ion species.

Two ideas need to be developed, to handle the chemistry effects. One approach is to improve the vacuum by an order of magnitude, to the pTorr range. Another approach is to figure out how to heat up the antiprotons enough to high temperatures where the cross sections<sup>11</sup> are in the kbarn range. So far cyclotron heating has resulted in expulsion of ions from the trap. The trick will be to figure out how to apply just enough heating to suppress charge-exchange (or antiproton-atom formation), but not too much to avoid expulsion.

## Summary

The main thrust of the trap development was to diagnose the behavior, identifying techniques which can be used for trapping holding and extracting antiprotons.

A technique involving a rotating wall RF technique, similar to that developed at UCSD, is expected to be applicable to the storage of antiprotons. While the technique appears to have the radial diffusion processes under control, the chemistry problems will require improvements in the quality of the vacuum.

Key items addressed over the past year include the following:

- Control of Penning discharge with spoiler screens;
- Particle identification by cyclotron resonance;
- Manipulation of energy states obtained upon extraction;
- Extend lifetime of ions using RF excitation of cloud rotation;
- Identify need for improvements in vacuum quality, RF pickup, and simulation including plasma effects.

## Appendix 1 – beamline simulation

The trapping process involves the motion of particles in external electric and magnetic fields. A Fortran program (TRAPEX) written for these simulations is based on TRANSPORT<sup>12</sup> and EGUN<sup>13</sup>.

The figure below illustrates a typical result from TRAPEX, in this case used in the design of the 90° bending magnet for the electron beam. By adjusting the tilt and orientation and displacement of the coils, the beam is focused in both the bend-plane and non-bend-plane by the fringe field.

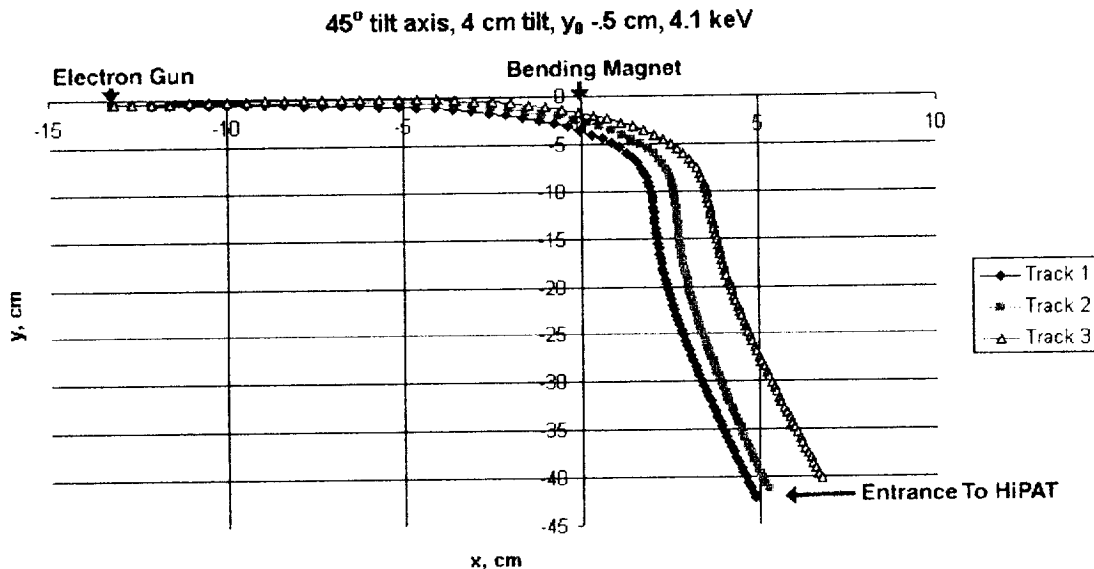


Figure 14 Bend-plane projection of electron trajectories.

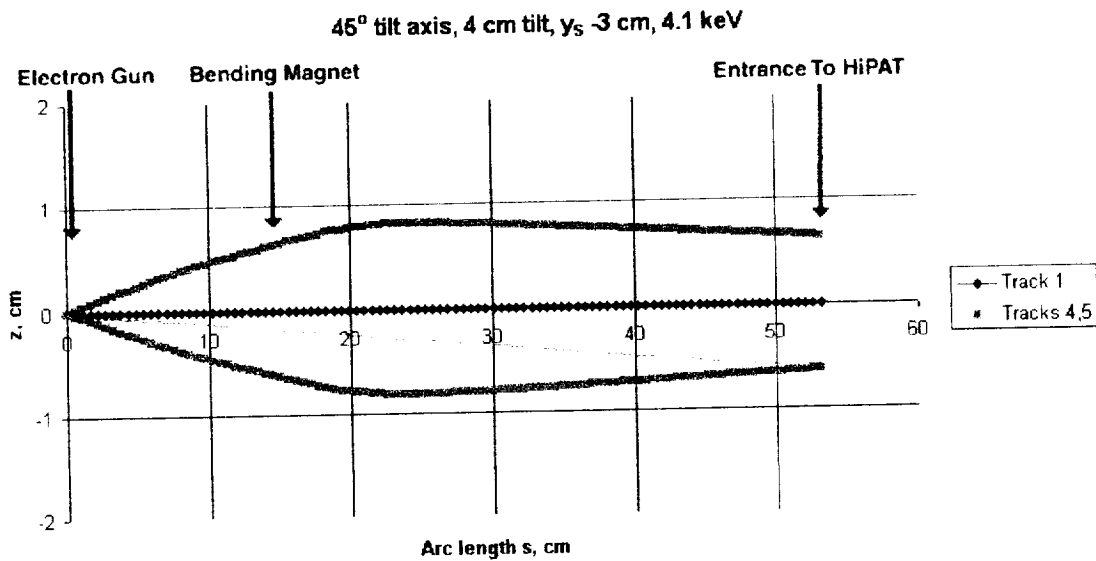


Figure 15 Non-bend-plane projection of electron trajectories.

The electron transport system works, with the magnet currents and configuration used in the simulations. However the simulation program generally overestimates the energy of ions extracted from the trap. A more elaborate code, taking into account inter-particle (plasma) effects, is needed to explain effects such as the energy clustering.

- <sup>1</sup> X.-P. Huang, F. Anderegg, E.M. Hollmann, T.M. O'Neil and C.F. Driscoll, *Phys. Rev. Lett.* 78, 875, 1997.
- <sup>2</sup> D.J. Wineland and H.G. Dehmelt, *J. App. Phys.* 46 (2), 919, 1975.
- <sup>3</sup> T. Simko, V. Marusovitz, T. Bretagne and G. Gousset, *Phys. Rev. E* 56, 5908, 1997, and G. Jiang et al., *Chem. Phys. Letters* 284,267, 1998.
- <sup>4</sup> G. Gabrielse et al., *Phys. Rev. Letters* 65, 1317, 1990.
- <sup>5</sup> G. Bollen et al., *Isoltrap*, *Nucl. Inst. And Meth. A* 368, 675, 1996.
- <sup>6</sup> L.S. Brown and G. Gabrielse, *Geonium theory*, *Rev. Mod. Phys.* 58 (1), 233, 1986.
- <sup>7</sup> E. Sarid, F. Anderegg and C.F. Driscoll, *Cyclotron resonance phenomena in a non-neutral multispecies ion plasma*, *Phys. Plasmas* 2 (8), 2895, 1995.
- <sup>8</sup> T.M. O'Neil, *Centrifugal separation of a multispecies pure ion plasma*, *Phys. Fluids* 24(8), 1447, 1981.
- <sup>9</sup> E.M. Hollmann, F. Anderegg and C.F. Driscoll, *Physics of Plasmas* 7(7), 2776, 2000.
- <sup>10</sup> M. H. Holzschneider, X. Feng and R.A. Lewis, *Hyperfine Interactions* 103, 377, 1996.
- <sup>11</sup> W.R. Gibbs, *Phys. Rev. A* 56(5), 3553, 1997.
- <sup>12</sup> D.C. Carey and K.L. Brown, *TRANSPORT*, SLAC-91, 1983.
- <sup>13</sup> W.A. Herrmannsfeldt, *EGUN*, SLAC-331, 1988.